Hindawi
Shock and Vibration
Volume 2021, Article ID 6629888, 14 pages
https://doi.org/10.1155/2021/6629888

Research Article

A Study of Safety Coefficient Determination and Support Parameter Optimization Based on Vulnerability Preevaluation

Minglei Zhang,[1,2] **Linsheng Gao**,[3] **Yue Yang**,[3] **Yidong Zhang**,[4] **and Ming Ji**[4]

[1]*Institute of Disaster Prevention, Hebei Key Laboratory of Earthquake Disaster Prevention and Risk Assessment, Langfang 065201, China*
[2]*Key Laboratory of Building Collapse Mechanism and Disaster Prevention, China Earthquake Administration, Langfang 065201, China*
[3]*North China Institute of Science and Technology, Langfang 065201, China*
[4]*School of Mine, China University of Mining and Technology, Xuzhou 221116, China*

Correspondence should be addressed to Linsheng Gao; gaolinsheng@ncist.edu.cn

Received 23 December 2020; Accepted 16 May 2021; Published 25 May 2021

Academic Editor: Roger Serra

The preevaluation to the vulnerability of the surrounding rocks is proposed as one of the reliable indicators of the safety coefficient of gateway support and a foundation to optimize the support design parameters. In this study, taking the surrounding rocks, stress, geological environment, and service time into consideration, the safety coefficient is determined based on the vulnerability scores calculated by the vulnerability preevaluation model of the surrounding rock. Applying the safety coefficient to the instability evaluation of the composite rock-bolt bearing structure, the strength required to maintain the stability of the gateway is calculated, which further provides references and guidance to the optimization of the anchor support parameters. This method has been successfully adopted by the GuCheng coal mining project in N1303 tailgate to strengthen the anchor-bolt structure in the roof watering area especially the main inclined shaft. Applying more accurately calculated strength to the anchor-bolt structure can effectively avoid the issue of overcompensation, thus reducing the cost and increasing the driving speed. Furthermore, this method provides insights into optimizing design parameters of the gateway. This method provides a reliable basis for the optimization design of bolt support parameters in coal mine gateway.

1. Introduction

Due to the influence of complex natural stress field in the surrounding rock, deep mining will face more intricate engineering rock mechanics problems than shallow mining [1]. Generally speaking, the limit of the transition from shallow to deep is called the limit depth, and the gateway whose depth exceeds the limit depth is called a deep gateway. The surrounding rock support of gateways above the limit depth is relatively simple and easy to maintain, but it is relatively difficult below. With the increase of mining depth, high stress environment, soft rock, large deformation, and other issues affect the stability of roadway surrounding rock and threaten the safety production of coal mine [2]. Therefore, many support methods, such as steel support, anchor rod, anchor cable, and shotcrete, are applied to the surrounding rock control of the deep gateways. In particular, bolt support, due to the advantages of good support effect, low support cost, simple technology, and low labor intensity, has gradually become the main means of coal mine gateway support.

As a key in bolt support of coal mine gateway, reasonably designed support parameters can maximize the advantages of bolt support and achieve the safety of gateway. Due to the complex underground geological environment, a safety coefficient is often included in the anchor design to ensure the safety construction. However, the safety coefficient is usually identified based on the empirical value. This approach is featured with randomness [3]. An overly high safety coefficient tends to lead to an unnecessarily high

support strength, jeopardizing the construction progress and increasing the cost accordingly. On the other hand, an underestimated safety coefficient can result in insufficient bolt support strength, risking the construction safety [4]. Therefore, it is of great significance to select a reasonable safety coefficient for the purpose of efficient operation of anchor bolts and construction safety [5].

Generally speaking, the determination of the safety coefficient of the gateway needs to refer to the damage degree of the surrounding rock of the gateway, which can be expressed by the degree of vulnerability [6]. Vulnerability can be used to describe the vulnerability of relevant systems and their components. Insufficient bearing capability will degrade the system to its original state [7]. Furthermore, vulnerability is often considered and analyzed together with sensitivity and stability in the field of underground gateway engineering [8–11]. However, under most of cases, qualitative results are often drawn from the analysis. Since the gateway stability evaluation fails to correlate with the support parameters of the surrounding rock directly, it can only provide qualitative guidance to the gateway support parameters design and optimization instead of quantitative calculation guidance. Meanwhile, the optimization of the gateway support tends to occur in the case of major gateway deformation observed, which easily attracts the attention of researchers [12–14]. However, for gateways with small deformations, due to various safety risk concerns and the lack of quantitative evaluation methods, reducing the excess support strength is often overlooked with little optimization. Maintaining the status quo is preferred by the authorities. This mindset and approach slow down the excavation speed and increase the cost related to the supporting system, jeopardizing the goal of high production and efficiency.

In this paper, the preevaluation to the vulnerability of the surrounding rocks is proposed as one of the reliable indicators of the safety coefficient of gateway support and a foundation to optimize the support design parameters. Taking the surrounding rocks, stress, geological environment, and service time into consideration, a vulnerability preevaluation model is established through the analytic hierarchy process method. Following the theory of composite rock-bolt bearing structure, the bolt support parameters are identified through the quantitative calculation. The proposed approach has been applied to the gateways with both major deformations and small deformations, proving to be effective in reducing overly estimated bolt support strength.

2. Instability Criterion of Composite Rock-Bolt Bearing Structure

In order to maintain the stability of the surrounding rock stable, preloaded bolts are installed to reinforce the roof and two ribs of gateway. The preloaded bolts of proper dimensions and materials, together with the supporting accessories, form a bearing structure to the gateway surrounding rock, providing some strength and bearing capability. The geometric form of composite rock-bolt bearing structure is shown in Figures 1(a) (arch) and 1(b) (rectangle).

The strength of composite rock-bolt bearing structure can be calculated by [15, 16]

$$q = p_i\left(\frac{1+\sin\varphi}{1-\sin\varphi}A_1 + A_2\right) + \left(\frac{2c\cos\varphi}{1-\sin\varphi}A_1 + A_3\right), \quad (1)$$

$$p_i = \frac{\pi d^2 \sigma_b}{(4C_S R_s)}, \quad (2)$$

where p_i is the bolt support strength, d refers to the diameter of bolt, σ_b indicates the tensile strength of bolt, C_s stands for the column spacing of bolt, and R_s shows the row spacing of bolt.

If the gateway shape is arch, $A_1 = b/(R+b)$, $A_2 = R/(R+b)$, $A_3 = b^2/(4(R+b))$, where R means the radius of arch gateway, and b indicates the thickness of composite rock-bolt bearing structure, which can be calculated by the sum of the thickness of internal nonuniform compression band (b_0) and the thickness of uniform compression band b_1. Bolt length is supposed to be l. $b_0$and $b_1$can be calculated by

$$b_0 = \max\frac{(C_s, R_s)}{2}, \quad (3)$$

$$b_1 = l - \max(C_s, R_s). \quad (4)$$

If the gateway shape is arch, $A_1 = 2b/(R_1(1-\cos\beta))$, $A_2 = B/(R_1(1-\cos\beta))$, $A_3 = b^2/(2R_1(1+\cos\beta))$, where R_1stands for the outer boundary curve radius of composite rock-bolt bearing structure for rectangle gateway, β is the center angle corresponding to outer boundary curve of composite rock-bolt bearing structure for rectangle gateway, and B indicates the width of gateway. R_1 and β can be calculated by

$$R_1 = b + \left(\frac{B}{2}\right) + \left(\frac{B^2}{8b}\right), \quad (5)$$

$$\beta = 2\arcsin\left(\frac{B}{2} + \frac{b}{R_1}\right). \quad (6)$$

The gateway strata weight is mainly borne by the deep surrounding rock, while the formed composite rock-bolt bearing structure mainly bears the weight of the loose strata of the gateway. According to the field damage conditions of the underground gateway and related research, when the external load exceeds the strength of the composite rock-bolt bearing structure, serious roof falling and excessive deformation will be observed in the gateway. Therefore, in order to ensure the stability of the composite rock-bolt bearing structure during the service life of the gateway, calculating the weight of the potential loose overlying rocks and determining the external load borne by the composite rock-bolt bearing structure become crucial. According to the relevant researches, the thickness h of the potential loose rock layer of the gateway roof is calculated as follows [17]:

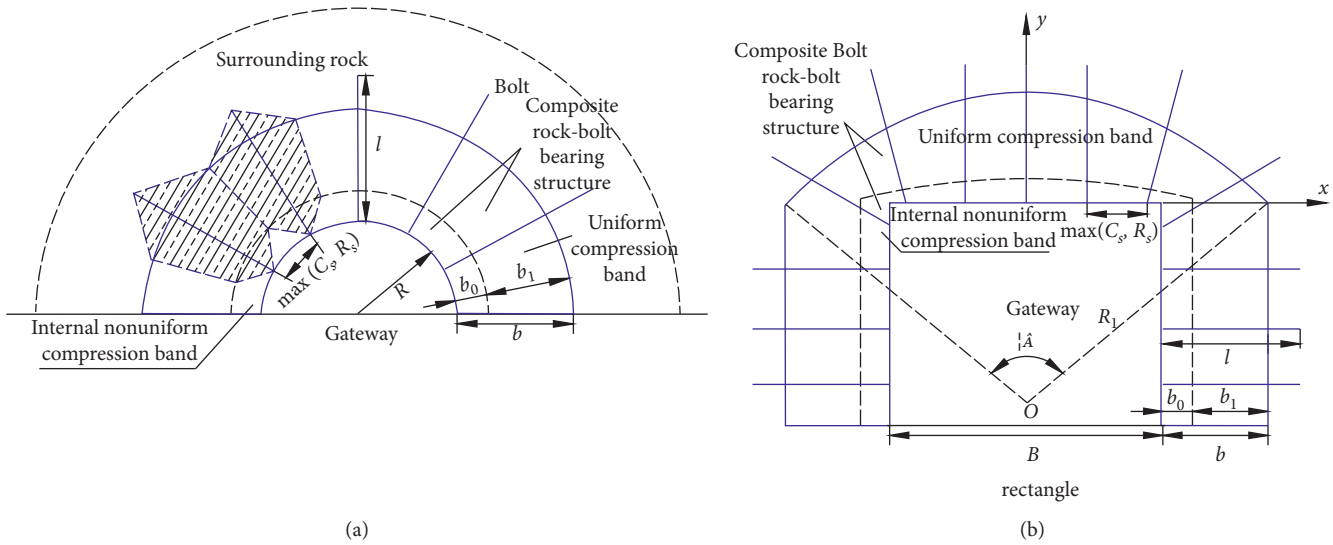

Figure 1: Geometric form of composite rock-bolt bearing structure: (a) arch; (b) rectangle.

$$h = \frac{B\tan((\pi/4)-(\phi/2)) + H\left[\lambda + \tan^2((\pi/4)-(\phi/2))\right]}{2\lambda} + \frac{\sqrt{(B/2)^2 + l^2}}{\sqrt{\lambda}} - H, \tag{7}$$

where φ is the internal friction angle of the roof stratum, and λ refers to the lateral pressure coefficient.

Following the method mentioned above, the evenly distributed load on the composite rock-bolt bearing structure is calculated, and its strength is tested. When the upper evenly distributed load is less than the strength of the composite rock-bolt bearing structure, the composite rock-bolt bearing structure is stable with limited displacement. Under the event that the upper evenly distributed load is greater than the load limit of the composite rock-bolt bearing structure and a low shrinkage of the bearing structure, the bearing structure tends to fail, resulting in the gateway roof collapse. On the other hand, a bearing structure with a high shrinkage rate can cause dramatic deformation and eventually lead to the gateway failure. Considering a reasonable safety coefficient, the instability evaluation of composite rock-bolt bearing structure should be based on

$$q \geq n\gamma h, \tag{8}$$

where n refers to the safety coefficient, whose value is determined by the vulnerability preassessment of the gateway surrounding rock.

When $q < n\gamma h$, the composite rock-bolt bearing structure is most likely to fail during the service period. However, due to volatility of the geological conditions, drastic deformations occur more commonly to the bearing structure.

3. Determination of the Safety Coefficient Based on Vulnerability Preevaluation

3.1. The Establishment of the Vulnerability Evaluation System

3.1.1. The Vulnerability Evaluation System and Indicators. According to the analysis on the factors that affect the vulnerability of the gateway surrounding rocks, the indicators are selected to evaluate the vulnerability of the gateway surrounding rocks. Based on the Analytic Hierarchy Process (AHP) [9], the indicators were divided into three levels, as shown in Figure 2.

The scores and evaluation level are listed below:

(1) Scores for the characteristics of the surrounding rocks

(i) The integrity of the surrounding rocks
The integrity of the surrounding rocks can be influenced by the number of rock planes, shape, spacing, and roughness of the surrounding rock structure. The surrounding rock integrity is rated based on RQD for various integrity level and shown in Table 1.

(ii) The strength of the surrounding rocks
The roof rock mass strength, side rock mass strength, and floor rock mass strength are important factors to evaluate the stability of the surrounding rock. The strength of the surrounding rock is indicated by the uniaxial

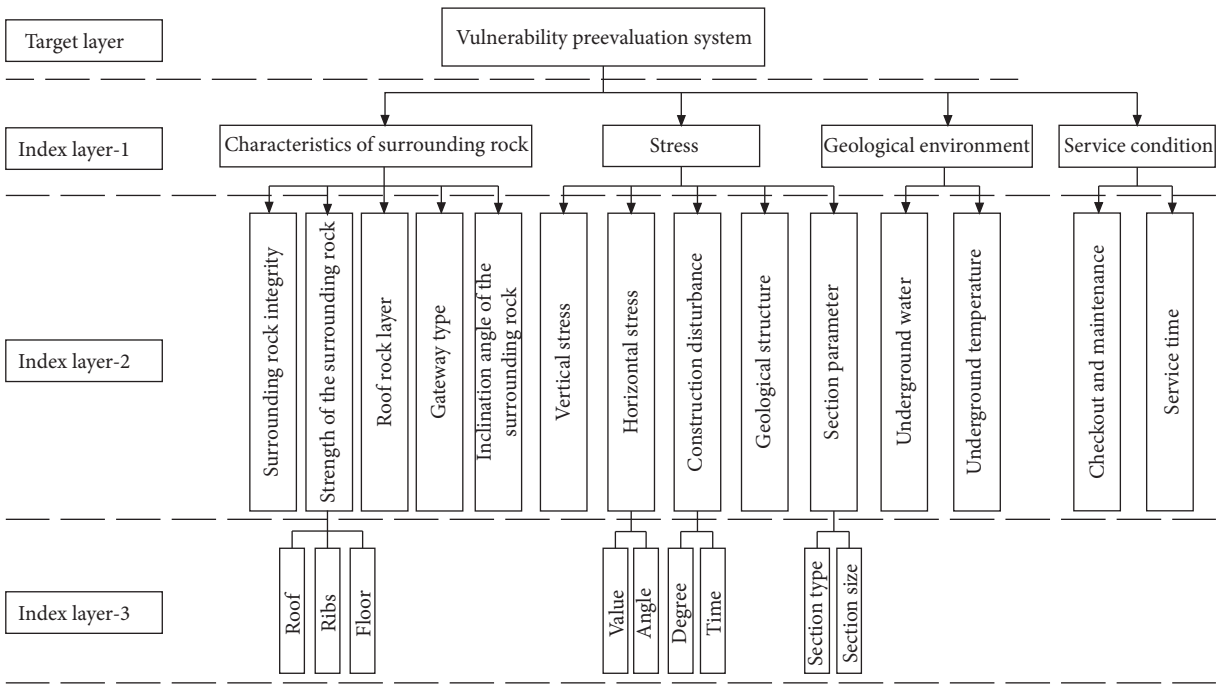

Figure 2: The preevaluation indexes of the surrounding rock vulnerability.

compressive strength of the roof rock mass. The surrounding rock strength is rated and presented in Table 2.

(iii) Roof rock layer
The reinforcement effect of the bolts varies depending on various rock layers, such as the rock roof, coal roof, and composite roof, making the rock layer an important factor to evaluate the roof stability. The impact of the rock layer characteristics on the stability evaluation is rated and presented in Table 3.

(iv) Gateway type
The gateway type refers to the combination of various surrounding rocks of the gateway including the rock gateway, the coal gateway, and the semicoal gateway. The gateway type is rated and presented in Table 4.

(v) The inclination angle of the surrounding rock
The inclination angle of the surrounding rock is considered as one of the important factors to evaluate the vulnerability of the gateway surrounding rock, which is rated and presented in Table 5.

(2) The stress

(i) The vertical stress
The vertical stress is a fundamental factor to the deformation and failure of the gateway surrounding rock. The vertical stress is rated by the buried depth and presented in Table 6.

(ii) The horizontal stress

Table 1: The scores of the surrounding rock integrity.

RQD (%)	100 ~ 80	80 ~ 60	60 ~ 40	40 ~ 20	20 ~ 0
Scores	2	4	6	8	10

Table 2: The scores of the surrounding rock uniaxial compression strength.

Strength of roof (MPa)	>80	80 ~ 60	60 ~ 40	40 ~ 20	20 ~ 0
Scores	2	4	6	8	10

Table 3: The scores of roof characteristics.

Roof type	Rock roof	Coal roof	Composite roof
Scores	3	6	9

Table 4: The scores of gateway types.

Gateway type	Rock gateway	Semicoal gateway	Coal gateway
Scores	3	6	9

Table 5: The scores of the inclination angles.

The inclination angle (°)	0 ~ 8	8 ~ 25	25 ~ 45	>45
Scores	2.5	5	7.5	10

Table 6: The score of the buried depths.

Depth (m)	<100	100 ~ 300	300 ~ 500	500 ~ 700	>700
Scores	2	4	6	8	10

The influence of horizontal stress on the surrounding rock can be represented by the maximum principle horizontal stress and the angle between the axis of the gateway and the orientation of the maximum principal horizontal stress, which are often considered as key factors to evaluate the stability of the gateway surrounding rocks. The maximum horizontal principal stress and the angle between the gateway axis and maximum principal horizontal orientation are rated and presented in Tables 7 and 8, respectively.

(iii) The construction disturbance

During the service period of gateway, the surrounding rock vulnerability is affected by the disruptions generated by the excavation or mining [18]. During the excavation, the width of the protective coal pillar often leads to the stress redistribution, which can be used to indicate the disruption received by the surrounding rocks.

The abutment pressure σ_z was considered to consist of stress increment ($\sum \sigma_i$) and geostatic stress (σ_q), as shown in Equations (9)–(11) [19].

$$\sigma_z = \sum \sigma_i + \sigma_q, \tag{9}$$

where $\sigma_i\,(i = 1 - n)$is for the abutment stress transmitted from the suspended part of a key layer to solid coal, and n refers to the number of key layers.

$$\sigma_i = \begin{cases} \dfrac{\sigma_{i\max} x \tan\alpha}{H_i}, & \left(0 < x < \dfrac{H_i}{\tan\alpha}\right), \\ 2\sigma_{i\max}\left(1 - \dfrac{x\tan\alpha}{2H_i}\right), & \left(\dfrac{H_i}{\tan\alpha} \le x < \dfrac{2H_i}{\tan\alpha}\right), \\ 0, & \left(x > \dfrac{2H_i}{\tan\alpha}\right), \end{cases} \tag{10}$$

$$\sigma_q = \begin{cases} \gamma I, & \left(0 < x < \dfrac{I}{\tan\alpha}\right), \\ \gamma x \tan\alpha, & \left(\dfrac{I}{\tan\alpha} \le x < \dfrac{H_i}{\tan\alpha}\right), \\ \gamma H, & \left(x > \dfrac{H_i}{\tan\alpha}\right), \end{cases} \tag{11}$$

where $\sigma_{i\max}$ is the maximum abutment stress transmitted from the suspended part of ith key layer to solid coal, $\sigma_{i\max} = Q_i/H_i \cot\alpha$, $Q_i$is the gravity of half of the suspended part of ith key layer, $Q_i = L_i M_i \gamma/2L_i$ refers to the suspended length of the center line of ith key layer in thickness direction,$\gamma L_i = 2I + 2H_i \cot\alpha$indicates the strata bulk density, M_i is the thickness of ith key layer, $H_i$means the distance from coal floor to the center line of ith key layer in thickness direction, $H_i = I + M_i/2 + \sum M_i\,(j = 1 - i - 1)I$ refers to half of the gob width, and $H$is the buried depth of coal.

According to Equations (9)–(11) and curve of abutment pressure distribution shown in Figure 3, the stress on the solid coal was divided into four parts, and the vulnerability of gateways driven in different areas was listed from low to high: IV < I < III < II [19]. Besides, retaining gateway along gob (pillar width is 0 m) was considered as a specific condition without coal pillar and was more difficult to control the stability of surrounding rock [20]. The construction disturbance degree is rated by the protective pillar widths and presented in Table 9. The scores corresponding to various states of disturbance times are shown in Table 10.

(iv) Geological Structure

Common geological structures in coal mine include folds, faults, and collapse columns. The influence of geological structure on the surrounding rock is evaluated based on the quantity and scale of geological structures within a radius of 50 m around the area to be assessed [21]. The scale of structure is rated into three levels, small (S), medium (M), and large (L). The scores of various geological structures are shown in Table 11.

(v) Section parameter

The section parameter comprises the section type and section size, which exert significant impact on the stress distribution and stress concentration of the gateway surrounding rock. The scores for the section type and section size are shown in Tables 12 and 13 separately.

(3) Geological Environment

(i) Underground water

Water accumulations in the boreholes degrade not only the strength of the anchor bolts, but also the strength of the surrounding rock, which jeopardizes the stability of the gateway surrounding rock. Besides, due to the softening property, the inhaled water tends to degrade the rock strength [22]. The scores of the groundwater are shown in Table 14.

(ii) Underground temperature

The temperature around the borehole can influence the resin anchor-hold [23]. The scores of the underground temperature are provided in Table 15.

(4) Service time

(i) Inspection and maintenance

Inspection and maintenance are among important methods to detect and solve problems in time. Manual monitoring means inspections conducted mainly through manpower. Machine monitoring indicates that the monitoring and recording are

Table 7: The scores of maximum principal horizontal stresses.

Major horizontal principal stress (MPa)	<8	8 ~ 16	16 ~ 24	24 ~ 36	>32
Scores	2	4	6	8	10

Table 8: The scores of included angles between gateway axis and major horizontal principal stress.

Included angle (°)	0 ~ 18	18 ~ 36	36 ~ 54	54 ~ 72	72 ~ 96
Scores	2	4	6	8	10

Table 9: The scores of width of protective pillar in the current coal seam.

Width of the protective coal pillar	IV	I	III	II	0 m
Scores	2	4	6	8	10

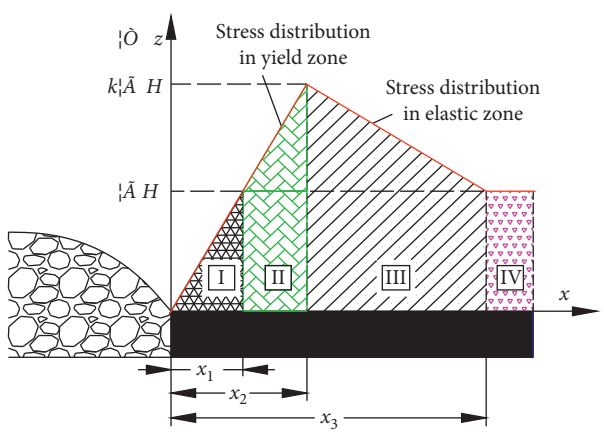

Figure 3: Stress redistribution on the solid coal along the gob [20] (I: destressed yield zone $(0 < x \leq x_1)$, II: overstressed plastic zone, $(x_1 < x \leq x_2)$, III: overstressed elastic zone $(x_2 < x \leq x_3)$, and IV: premining vertical stress zone $(x > x_3)$).

conducted by machines and auto systems, such as borehole stress meters, deep displacement meters, and data storage equipment. Smart monitoring indicates the smart data monitoring and analysis [24]. The scores of inspections and maintenance are shown in Table 16.

(ii) Service time
With the increased service time, the gateway surrounding rock often develops the creep deformation, which escalates the internal damage, resulting in higher vulnerability of the gateway surrounding rock [25]. The scores of service time are shown in Table 17.

3.1.2. Confirmation of Weighted Values. (1) Calculation Steps. Taking expertise of various experts into consideration, according to the principles of AHP, a judgement matrix was developed. E is defined as the comparative matrix, as shown in

$$E = \begin{bmatrix} E_{11} & E_{12} & \dots & E_{1j} \\ E_{21} & E_{22} & \dots & E_{2j} \\ \dots & \dots & \dots & \dots \\ E_{i1} & E_{i2} & \dots & E_{ij} \end{bmatrix}. \quad (12)$$

In the judgement matrix, E_{ij}refers to the ratio between magnitude $E_j$and magnitude $E_j$under condition E:

$$E_{ij^{\cdot}} = \frac{E_i}{E_j}, \quad (13)$$

where $E_i$is to evaluate the ith factor, and $E_j$is to evaluate the jth factor, and $E_{ji} = E_j/E_i = 1/E_{ij}$.

Factors E_i and $E_jE_j$are evaluated and compared via the judgement matrix by following a 1–9 scale method, as shown in Table 18.

Thirdly, both maximum eigenvalues $\lambda_{\max}$ and the corresponding eigenvectors included in the judgement matrix were calculated via MATLAB software.

Fourthly, a judgement matrix consistency test was conducted. Since both subjective and approximate evaluations are included during the development of the judgement matrix, deviations are possible. Thus, a consistency test is required. The CR ratio can be calculated by

$$\mathrm{CR} = \frac{\mathrm{CI}}{\mathrm{RI}}, \quad (14)$$

where CR is the consistency ratio, CI represents the consistency indicator, $\mathrm{CI} = (\lambda_{\max} - t)(\lambda_{\max} - t)/(t-1)t$ displays the order of the matrix, and RI refers to the mean random consistency index, which is shown in Table 19.

Both CI and CR must be below 0.1 [22–25].

Lastly, the weight of each indictor was calculated. After the consistency test, the weight values were determined by following the steps listed in Figure 4.

(2) Calculation Results. In order to demonstrate the weight value calculation process, the indicators for layer-1 are explained in detail below. The judgement matrix built is shown as

$$E = \begin{bmatrix} 1 & 1 & 4 & 1 \\ 1 & 1 & 5 & 2 \\ \frac{1}{4} & \frac{1}{5} & 1 & 1 \\ 1 & \frac{1}{2} & 1 & 1 \end{bmatrix}. \quad (15)$$

Table 10: The scores of disturbance times from mining.

Disturbance times	$1e$	$2e$	$3e$	$1e + 1m$	$2e + 1m$	$1e + 2m$	$2e + 2m$	Others
Scores	2	3	4	5	6	7	8	10

"e" denotes "excavation disturbance" and "m" refers to "mining disturbance". "$1e$" indicates the gateway suffering once excavation distribution, while "$2e$ and $1m$" mean the gateway suffering twice excavation distribution and once mining distribution.

Table 11: The scores of geological structures.

Geological structure	None	S	M	$2S$	$1S + 1M$	$2S + 1M$	L	$2M$	$1S + 2M$	Others
Scores	1	2	3	4	5	6	7	8	9	10

Table 12: The scores of section type.

Section type	Circular	Arch	Straight wall semicircle arch	Trapezoid	Rectangle
Scores	2	4	6	8	10

Table 13: The scores of section size.

Section size (m^2)	<14	14 ~ 17	17 ~ 19	19 ~ 21	>21
Scores	2	4	6	8	10

Table 14: The scores of water pouring amount.

Water pouring amount (ml/min)	<100	100 ~ 350	350 ~ 500	500 ~ 650	>650
Scores	2	4	6	8	10

Table 15: The scores of underground temperatures.

Ground temperature (°)	<20	20 ~ 40	40 ~ 60	60 ~ 80	>80
Scores	2	4	6	8	10

Table 16: The scores of service time.

Inspection and maintenance	None	Manual monitoring	Machine monitoring	Smart monitoring
Scores	10	7.5	5	2.5

Table 17: The scores of service time.

Service time (y)	<5	5~15	15~30	30~45	>45
Scores	2	4	6	8	10

Table 18: 1–9 scaling method.

The ratio of factors	Quantized values	The ratio of factors	Quantized values
Equally important	1	Highly important	7
Somewhat important	3	Extremely important	9
Important stronger	5	Intermediate value between two adjacent judgments	2, 4, 6, 8

The highest eigenvalue of judgement matrix is $4.2365, \mathrm{CI} = (4.2365 - 4)/(4 - 1) = 0.078$, and $\mathrm{CR} = 0.078/0.9 = 0.087 < 0.1$. Thus, the judgement matrix meets the consistency requirement.

The weight matrix of the standard layer is $[0.31 \cdot 0.40 \cdot 0.10 \cdot 0.19]^T$ and the weights of other indexes calculated by AHP are shown in Table 20.

3.1.3. Vulnerability Evaluation. The value of a gateway surrounding rock's vulnerability evaluation can be calculated according to the weight listed in Table 19 and Eq. (16).

$$V_{j-1} = \sum_{i=1}^{n} s_{ij} w_{ij}, \tag{16}$$

Table 19: Value of RI.

Matrix order	1	2	3	4	5	6	7	8	9	10	11
RI	0	0	0.58	0.90	1.12	1.24	1.32	1.41	1.45	1.49	1.51

Table 19 is reproduced from Cheng et al. (2015) (under the Creative Commons Attribution License/public domain).

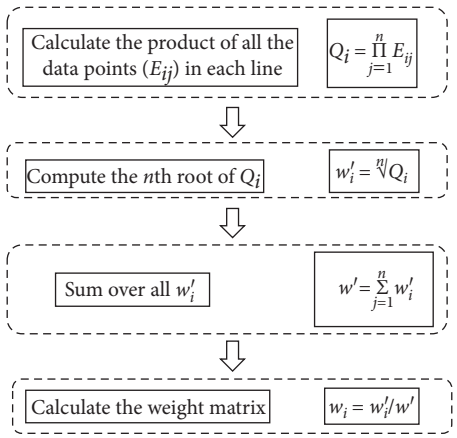

Figure 4: Steps to calculate weight values of indicators.

Table 20: The weights of the evaluation indexes.

Layer-1	Weight	Layer-2	Weight	Layer-3	Weight
Characteristics of the surrounding rock	0.31	Surrounding rock integrity	0.35		
		Strength of the surrounding rock	0.35	Roof	0.35
				Rib	0.4
				Floor	0.25
		Roof rock types	0.1		
		Gateway type	0.1		
		Dip angle of the surrounding rock	0.1		
Stress condition	0.4	Section parameter	0.1	Section type	0.5
				Section size	0.5
		Construction disturbance	0.35	Degree	0.5
				Time	0.5
		Geological structure	0.3		
		Buried depth	0.1		
		Major horizontal principal stress	0.15	Value	0.4
				Angle	0.6
Geological environment	0.1	Underground water	0.5		
		Underground temperature	0.5		
Service condition	0.19	Inspection and maintenance	0.2		
		Service time	0.8		

where V_{j-1} is the comprehensive score of layer-j, V_0 is the vulnerability score, s_{ij} is the evaluate score of ith factor in layer-j, and$w_{ij}$is the weight of ith factor in layer-j.

3.2. Vulnerability Score and Safety Coefficient. After calculating the vulnerability score, the vulnerability of surrounding rock can be rated into five levels. The corresponding safety coefficients are exhibited in Table 21.

4. Case Studies

4.1. The Case of Increasing the Density of the Bolt Support System. In order to examine the feasibility and effects of increasing the density of the bolt support, Gucheng coal mine of Luan Group, located in Shanxi Province, China, was selected. No water flooded into the tunnel when the main inclined shaft penetrated the soil surface and weathered bedrock section. However, after the main shaft entered into the bedrock section and reached certain depth, water was detected and even burst in the anchor boreholes. The anchor cable pull-out tests revealed that the anchor force dropped by nearly 32% and the anchor-hold was decreased by about 15%, which indicates that the water flooding and burst severely degraded the support for the main inclined shaft, resulting in a 100 mm deposition of the gateway roof with local cracks. This change significantly jeopardizes the 65-year designed gateway surrounding rock support.

Table 21: Classification standard for vulnerability of surrounding rock and safety coefficient.

Score	<3	$3 < V < 4$	$4 < V < 5$	$5 \leq V \leq 6$	$V > 6$
Vulnerability levels	I	II	III	IV	V
Safety coefficient	3.3	3.3~4	4~4.7	4.7~5.4	>5.4

Based on the survey and the field investigation to the boreholes and the drainage holes, two new aquifers were identified between gateway mileage points 580 m and 740 m. During the gateway construction, cracks were generated around the anchor cable when the cable went through the aquifer and the middle-layer surrounding rock, which allowed the water to flow out from the anchor cable boreholes ad anchor bolt boreholes. Due to the tight schedule and the lacking of the emergency response plan, the project supervisor decided to replace the anchor cable with the anchor support. Therefore, the vulnerability evaluation should be conducted to the gateway surrounding rock and develop optimization to the anchor bolt support parameters.

The evaluation parameters of the main inclined shaft are shown in Table 22. The main inclined shaft gateway penetrates different rock strata with a vertical depth of around 40 meters for this section. In order to ensure the gateway safety, the most unfavorable parameters to the stability of the rock strata are taken.

The main inclined shaft is jointly supported by anchor cable and a 150mm thick shotcrete. From the perspective of conservative estimation, without taking the bearing load of 150 mm thick shotcrete into account, the detailed parameters of the main inclined shaft are shown in Table 23.

According to Table 22 and Equation (11), the vulnerability score of the main inclined shaft is rated at 5.67, and the vulnerability preevaluation level is identified as IV with a safety coefficient of 5.2. The instability criterion for the main inclined shaft is illustrated as

$$q \geq 1.55\,\text{MPa}. \tag{17}$$

Based on the information listed in Table 23 and Equation (1), the strength of the composite rock-bolt bearing structure of the main inclined shaft is 1.5 MPa, which is below 1.55 MPa calculated by vulnerability preevaluation. This result is further validated by the increased deformation of the gateway roof and the cracks found in the shotcrete.

Based on the existing bolt types, reducing the distance among anchor bolts was recommended to increase the strength of the composite rock-bolt bearing structure. When the distance among anchor bolts was 824 mm, the strength of the composite rock-bolt bearing structure reached 1.55 MPa. Considering the safety construction, 800 mm was selected for the distance among anchor bolts, which provided 1.567 MPa as the composite rock-bolt bearing structure. The optimized supporting parameters can be viewed in Figure 5.

After the optimization, a deformation observation station is set at gateway mileage 594 m. As the deformation curve and the image of the completed optimization demonstrated in Figure 6, the control and support to the surrounding rock are improved. The observation for continuous 40 days suggests that the gateway roof deposition is 27 mm, and the heave at the bottom of the inclined shaft is measured at 6 mm. In addition, the deformation between two ribs is limited to 38 mm. The deformation rate grows lower on the eighth day after the excavation, indicating that the deformation of the main inclined shaft has been effectively controlled.

More specifically, water has a great impact on the safety of underground engineering, especially the long-term use of underground engineering. In order to further reduce the influence of water on the stability of surrounding rock, the grouting reinforcement measure was applied in the main inclined shaft. Parameters and effect of grouting reinforcement are shown in Figure 7.

4.2. The Case of Reducing Bolt Support Density. N1303 working face is located at Gucheng No. 1 mining zone, which mainly mines Coal seams #3 with a 6 m thickness through a fully mechanized caving technology. The tunnel for the conveyer in N1303 was excavated 600 m ahead the tailgate N1303. The deformation of conveyer tunnel is well controlled during excavation with low excavation speed (only 6.4 m/d), resulting in a high construction cost. Gateway layout of N1303 working face is shown in Figure 8.

In order to increase excavation speed and reduce the cost of the supporting system, the vulnerability preevaluation method was adopted to identify the safety coefficient of the tailgate N1303 and develop an optimization plan.

The evaluation parameters of tailgate N1303 are shown in Table 24.

The detailed parameters of tailgate N1303 are shown in Table 25.

According to Table 24 and Equation (11), the vulnerability score of tailgate N1303 is rated at 3.88, the vulnerability preevaluation level is identified as II, and the safety coefficient is 3.95. Therefore, the instability criterion of tailgate N1303 is expressed as

$$q \geq 0.969\,\text{MPa}. \tag{18}$$

Based on Table 25 and Equation (1), the strength of the composite rock-bolt bearing structure in tailgate N1303 is identified as 1.094 MPa, higher than the 0.969 MPa calculated by vulnerability preevaluation. Considering the existing bolt types, increasing the bolt column spacing and row spacing is recommended to lower the strength of composite rock-bolt bearing structure. With a 900 mm bolt row distance and a 1015 mm row spacing, the composite rock-bolt bearing structure strength reached 0.969 MPa. Considering the safety construction, 1000 mm was selected for the distance among anchor bolts, which provided 0.973 MPa as the composite rock-bolt bearing structure. The optimized supporting parameters can be viewed in Figure 9.

Table 22: Evaluation parameters and scores of the main inclined shaft.

Indictors	Value	Score	Indictors	Value	Score
Surrounding rock integrity (%)	52	6	Mining disturbance time	1	2
Roof strength (MPa)	25.48	8	Geological structure	2S	4
Rib strength (MPa)	25.48	8	Buried depth (m)	178	4
Floor strength (MPa)	25.48	8	Major horizontal principal stress (MPa)	3.2	2
Roof rock type	Rock	3	Angle between the axis of the gateway and the major horizontal principal stress (°)	42°	6
Gateway type	Rock	3	Underground water (ml/min)	600	8
Dip angle of the surrounding rock (°)	15	5	Underground temperature (°C)	17.3	2
Section type	Straight wall semicircle arch	6	Inspection and maintenance	Manual	7.5
Section size (m^2)	24.7	10	Service time	65	10
Pillar width (m)	∞	2			
Vulnerability score			5.67		
Vulnerability preevaluation level			IV		
Safety coefficient			5.2		

Table 23: Detailed parameters of the main inclined shaft.

	Parameter	Value	Dimension
Parameters of the surrounding rock	Cohesion	0.76	MPa
	Internal friction angle	17	(o)
Section size	Width	6400	mm
	Height	4400	mm
	Length	2400	mm
Bolt support parameter	Strength	335	MPa
	Diameter	22	mm
	Column spacing	800	mm
	Row spacing	900	mm

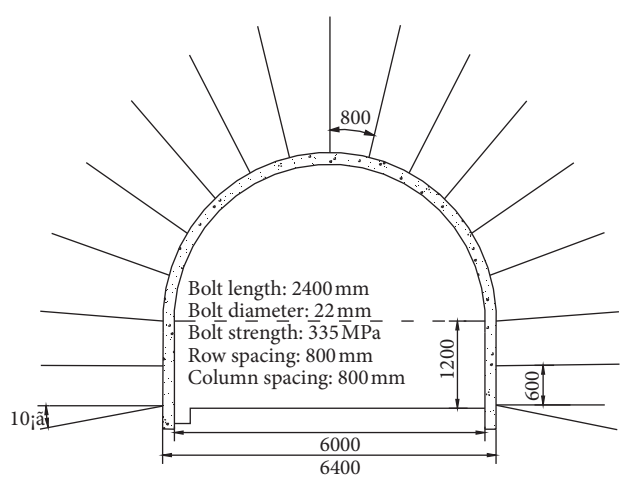

Figure 5: New support parameter of inclined shaft.

After the optimization, a deformation observation station A is set at mileage 50 m to measure the deformation during excavation period (as shown in Figure 10(a)), while an observation station B is set at mileage 1690 m to measure the deformation during mining period (as shown in Figure 10(b)).

The observation for continuous 40 days suggests that the tailgate N1303 roof deposition is 55 mm, and the heave at the tailgate bottom is measured at 6 mm. In addition, the deformation between two ribs is limited to 77 mm. The deformation rate grows lower on the tenth day after the excavation, indicating that the deformation of the tailgate N1303 has been effectively controlled.

As demonstrated in Figure 8(b), the deformation started to increase in the surrounding rock of the N1303 tailgate when the distance between the measuring station and the coal wall was at 93 m. When the distance was decreased to

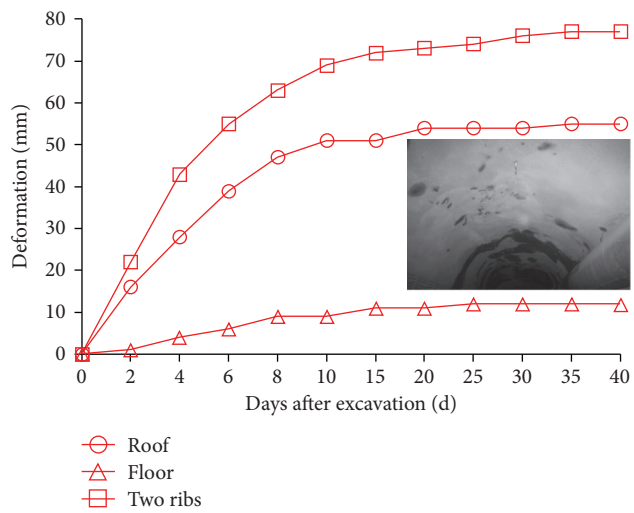

Figure 6: The deformation curve and the image of the completed optimization.

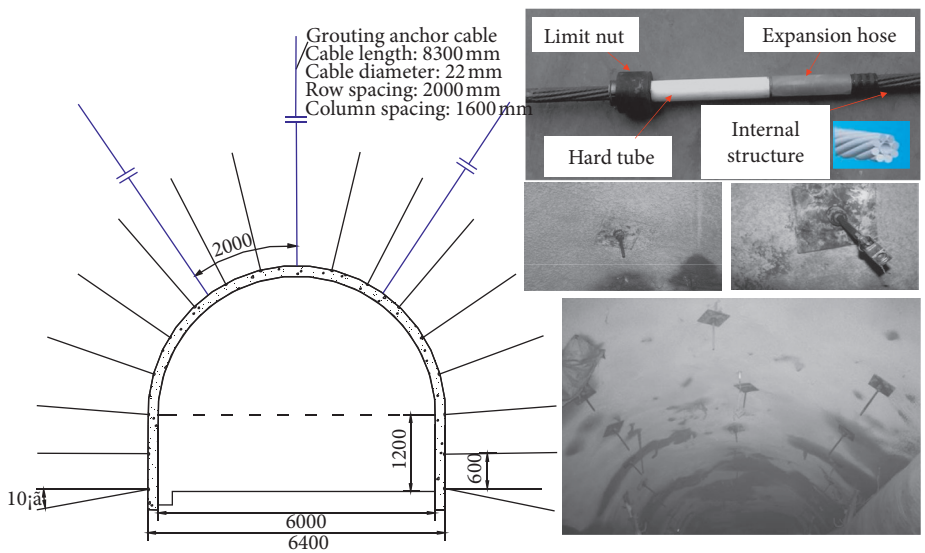

Figure 7: Parameters and effect of grouting reinforcement.

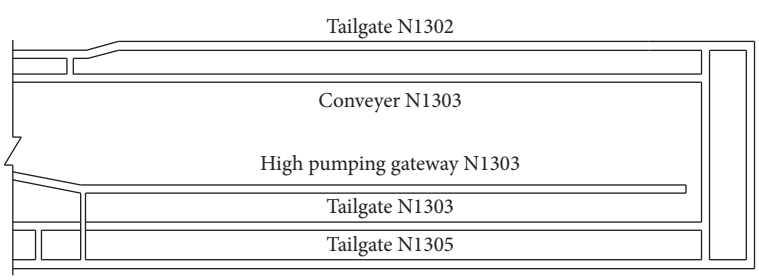

Figure 8: Gateway layout of N1303 working face.

35 m, the deformation increased drastically. During the excavation, the roof deposition reached 272 mm with a heave of 102 mm at the bottom. In addition, the deformation between two ribs is limited to 326 mm, suggesting that the deformation of the N1303 tailgate meets the desired specification.

The N1303 conveyer tunnel and tailgate N1303 are compared in Table 26 in terms of technology and economy.

As the data shows in Table 26, the total amount of roof deformation increased by 40.9%, the total amount of floor deformation increased by 92.4%, and the total amount of two ribs deformation increased by 35.2%. The average stress of bolt

Table 24: The evaluation parameters and scores of tailgate N1303.

Indictors	Value	Score	Indictors	Value	Score
Surrounding rock integrity (%)	83.5	2	Mining disturbance time	$1e+1$ m	5
Roof strength (MPa)	116.65	2	Geological structure	1S	2
Rib strength (MPa)	15.33	10	Buried depth (m)	490	6
Floor strength (MPa)	21.32	8	Major horizontal principal stress (MPa)	13.8	4
Roof rock type	Coal	6	Angle between the axis of the gateway and the major horizontal principal stress (°)	51	6
Gateway type	Coal	9	Underground water (ml/min)	25	2
Dip angle of the surrounding rock (°)	5	2.5	Underground temperature (°C)	18.9	2
Section type	Rectangle	10	Inspection and maintenance	Manual	7.5
Section size (m^2)	18	6	Service time (y)	3	2
Pillar width (m)	∞	2			
Vulnerability score			3.88		
Vulnerability preevaluation level			II		
Safety coefficient			3.95		

Table 25: Relevant parameters of tailgate N1303.

	Parameters	Value	Dimension
Parameters of surrounding rock	Cohesion	0.4	MPa
	Internal friction angle	21	(o)
Section size	Width	5000	mm
	Height	3600	mm
	Length	2400	mm
Bolt support parameter	Strength	335	MPa
	Diameter	22	mm
	Column spacing	800	mm
	Row spacing	800	mm

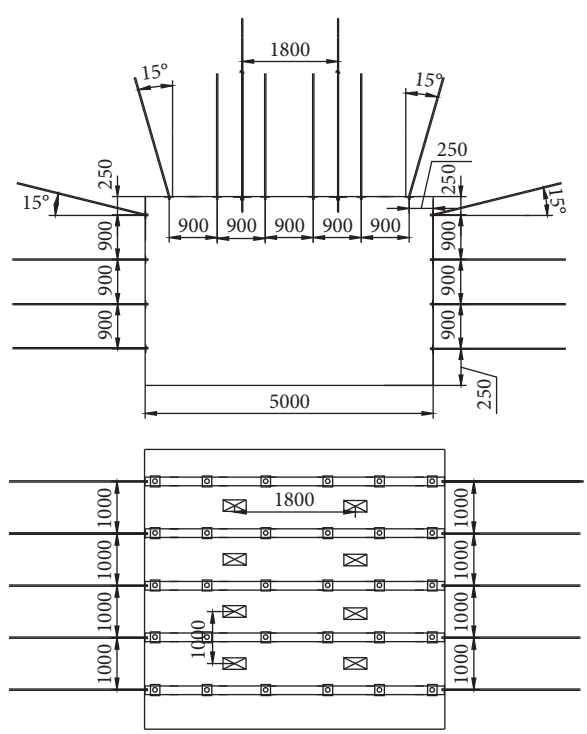

Figure 9: New support parameter of tailgate N1303.

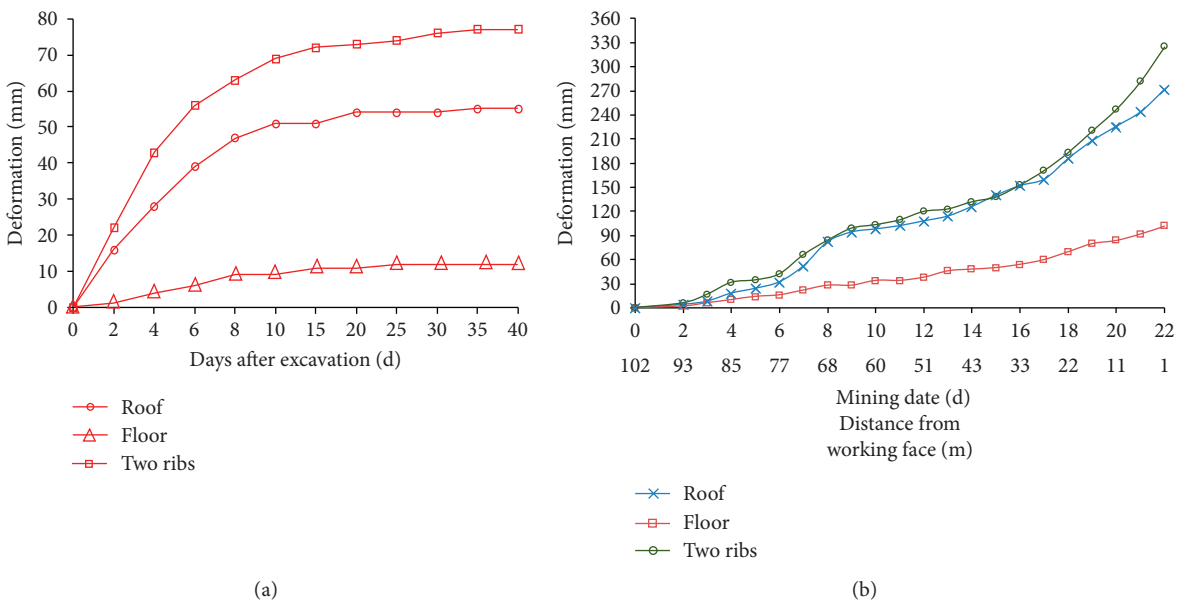

Figure 10: Deformation of gateway N1303 after support parameters optimization.

Table 26: The Comparison of N1303 conveyer tunnel and tailgate N1303.

Technical and economic indicators		Support parameter of N1303 conveyer tunnel	Optimization parameter in tailgate N1303	Difference
Total amount of deformation (mm)	Roof	193	272	+40.9%
	Floor	53	102	+92.4%
	Two ribs	241	326	+35.2%
Average stress during excavation(kN)	Bolt	63.4	98.6	+55.5%
	Anchor	115.6	235.8	104%
Excavation speed (m/d)		6.4	9	+40.6%
Cost (%)		100	74.6	−25.6%

during excavation increased by 55.5%, and the average stress of anchor during excavation increased by 104%. Although the percentage of growth is relatively large, the absolute value of growth is not large, and the total deformation of N1303 tailgate is still within the acceptable limit. In addition, after the optimization, the excavation speed increased by 40.6%, and the cost decreased by 25.6%. Therefore, the optimized support scheme can improve the driving speed and reduce the support cost on the premise of ensuring the gateway deformation.

5. Conclusion

(1) In this study, taking the surrounding rock, stress conditions, geological environment, and service time into consideration, a vulnerability preevaluation model is established by adopting the analytic hierarchy process.

(2) A vulnerability preevaluation method to the surrounding rock is proposed as the basis to evaluate the gateway support safety coefficient and optimize the design of the support system. The safety coefficient is obtained based on the vulnerability scores of the surrounding rock through the vulnerability preevaluation model. Applying the safety coefficient factor to the composite rock-bolt bearing structure for the instability evaluation, a required strength of the composite rock-bolt bearing structure can be identified quantitively with the optimization of the anchor bolt support.

(3) This method has been successfully adopted to optimize the anchor bolt support in the gateway water pool area of the main inclined shaft located in the Gucheng Coal Mine. The application suggests that this method can effectively maintain the stability of the surrounding rock and lower the support strength of the anchor bolt in N1303 tailgate, resulting in lower cost and increased excavation speed. This method provides reliable basis for the gateway bolt support optimization in coal mining industry.

Data Availability

The data used to support the findings of this study are available from the corresponding author upon request.

Conflicts of Interest

The authors declare that there are no conflicts of interest regarding the publication of this paper.

Acknowledgments

This work was supported by Self-Financing Project of Scientific Research and Development Plan of Langfang Science and Technology Bureau (Grant no. 2020013046), Scientific Research Found of Key Laboratory of Building Collapse Mechanism and Disaster Prevention, China Earthquake Administration (Grant no. FZ201207), and the Fundamental Research Funds for the Central Universities (Grant nos. 2020013046 and ZY20215156).

References

[1] C. J. Hou and L. S. Guo, *Coal Roadway Bolt Support*, China University of Mining and Technology Press, Xuzhou, China, 1999.

[2] W. J. Wang, E. Y. Dong, and C. Yuan, "Boundary equation of plastic zone of circular roadway in non-axisymmetric stress and its application," *Journal of China Coal Society*, vol. 44, no. 1, pp. 105–114, 2019, in Chinese.

[3] W. S. Zhao, L. J. Han, and Z. N. Zhao, "Influence of principal stress on surrounding rock stability of roadway intersection," *Rock and Soil Mechanics*, vol. 36, no. 6, pp. 1752–1760, 2015, in Chinese.

[4] L. K. Cheng, J. L. Fan, J. Han, and J. P. Xu, *Geotechnical Anchorage*, China Architecture & Building Press, Beijing, China, 2003.

[5] L. K. Cheng, Z. R. Zhang, and Z. Y. Yang, *Practical Technology of Geotechnical Reinforcement*, Earthquake Press, Beijing, China, 1994.

[6] S. R. Zhu, *Vulnerability Assessment Model and Application in Coal Enterprise*, Master's thesis, Henan University, Kaifeng, China, 2008.

[7] P. Timmerman, *Vulnerability Resilience and the Collapse of Society: A Review of Models and Possible Climatic Applications*, Institute for Environmental Studies University of Toronto, Toronto, Canada, 1981.

[8] M. Ji, H. J. Guo, Y. D. Zhang, L. Cheng, and Y. L. Ji, "Vulnerability analysis of soft caving gateway support system and surrounding rock optimal control technology research," *Mathematical Problems in Engineering*, vol. 2014, Article ID 987020, 12 pages, 2014.

[9] X. Y. Xiong, J. Dai, and X. Wang, "Comprehensive analysis of stability of coal seam composite roof based on analytic hierarchy process," *Advances in Civil Engineering*, vol. 20199 pages, Article ID 2042460, 2019.

[10] C. Y. Song, H. G. Ji, Y. J. Liu, and L. H. Sun, "Influencing neighboring factors of excavation disturbance on roadways in weakly cemented rock," *Journal of Mining and Safety Engineering*, vol. 33, no. 5, pp. 806–812, 2016, in Chinese.

[11] Z. Q. Zhang, D. M. Xu, and Q. S. Liu, "The research on the methodology of weighted average evaluation for surrounding rock stability of tunnel," *Rock and Soil Mechanics*, vol. 30, no. 11, pp. 3464–3468, 2009, in Chinese.

[12] H. P. Kang, J. Lin, and Y. Z. Wu, "High pre-tensioned stress and intensive cable bolting technology set in full section and application in entry affected by dynamic pressure," *Journal of China Coal Society*, vol. 39, no. 9, pp. 1153–1159, 2009, in Chinese.

[13] J. Yu, G. Y. Liu, Y. Y. Cai, J. F. Zhou, S. Y. Liu, and B. X. Tu, "Time-dependent deformation mechanism for swelling soft-rock tunnels in coal mines and its mathematical deduction," *International Journal of Geomechanics*, vol. 20, no. 3, 2020.

[14] X. Guo, X. Mao, C. Ma, and J. Huang, "Bolt support mechanism based on elastic theory," *International Journal of Mining Science and Technology*, vol. 23, no. 4, pp. 469–474, 2013, in Chinese.

[15] Y. D. Zhang, L. Cheng, J. F. Yang, M. Ji, and Y. H. Li, "Bearing characteristic of composite rock-bolt bearing structure under different bolt support density," *Journal of Mining and Safety Engineering*, vol. 32, no. 2, pp. 305–316, 2015, in Chinese.

[16] Y. D. Zhang, *Study on Bearing Characteristic of Composite Bolt-Rock Bearing Structure and Its Application in Roadway Bolting Design*, China University of Mining & Technology, Xuzhou, China, 2013, in Chinese.

[17] X. X. Miao, "Natural balance arch and stability of surrounding rock of tunnel," *Ground Pressure and Strata Control*, vol. 2, pp. 55–57, 1990, in Chinese.

[18] Z. Q. Zhang and J. S. Wei, "The research on the forecast of the influence of geological structures on surrounding rock stability," *Journal Taiyuan University Technology*, vol. 40, no. 2, pp. 177–179, 2009, in Chinese.

[19] J. H. Liu, F. X. Jiang, N. G. Wang, Z. S. Li, and Z. G. Zhang, "Research on reasonable width of segment pillar of fully mechanized caving face in extra-thick coal seam of deep shaft," *Chinese Journal of Rock Mechanical Engineering*, vol. 31, no. 5, pp. 921–927, 2012, in Chinese.

[20] Y. X. Zhao, Y. D. Jiang, K. X. Zhang, H. W. Wang, and S. P. Tian, "Analysis of gateway stability in underground coal mining based on disturbed state theory," *Journal of China University of Mining & Technology*, vol. 43, no. 2, pp. 233–240, 2014, in Chinese.

[21] J. Q. Jiang, J. S. Han, and Y. K. Shi, *Structure Stability of Gateways Surrounding Rock and Its Controlling Design*, China Coal Industry Publishing House, Beijing, China, 1998.

[22] S. Zhang, P. F. Gou, and H. Fan, "Influence of water and temperature on resin anchor-hold," *Journal of Southeast University*, vol. 35, no. S1, pp. 49–54, 2005, in Chinese.

[23] B. Hu, H. P. Kang, J. Lin, J. F. Cai, and P. F. Jiang, "Study on influence of temperature on anchorage performance of resin anchored bolt," *Journal of Mining and Safety Engineering*, vol. 12, no. 5, pp. 644–649, 2019, in Chinese.

[24] E. Y. Wang, *Real-time Monitoring and Early Warning Roadway Deformation Based on Machine Vision*, China University of Mining and Technology, Xuzhou, China, 2012.

[25] H. P. Kang and J. H. Wang, *Rock Bolting Theory and Complete Technology for Coal Roadways*, China Coal Industry Publishing House, Beijing, China, 2007.